In Chemotaxing Fibroblasts, Both High-Fidelity and Weakly Biased Cell Movements Track the Localization of PI3K Signaling

Citation: Melvin, Adam T., Erik S. Welf, Yana Wang, Darrell J. Irvine, and Jason M. Haugh. "In Chemotaxing Fibroblasts, Both High-Fidelity and Weakly Biased Cell Movements Track the Localization of PI3K Signaling." Biophysical Journal 100, no. 8 (April 2011): 1893–1901. © 2011 Biophysical Society.

As Published: http://dx.doi.org/10.1016/j.bpj.2011.02.047

Publisher: Elsevier

Persistent URL: http://hdl.handle.net/1721.1/92313

Version: Final published version: final published article, as it appeared in a journal, conference proceedings, or other formally published context

In Chemotaxing Fibroblasts, Both High-Fidelity and Weakly Biased Cell Movements Track the Localization of PI3K Signaling

Adam T. Melvin,[†] Erik S. Welf,[†] Yana Wang,[‡] Darrell J. Irvine,[§¶‖] and Jason M. Haugh[†*]

[†]Department of Chemical and Biomolecular Engineering, North Carolina State University, Raleigh, North Carolina; [‡]Department of Chemical Engineering, [§]Department of Materials Science and Engineering, and [¶]Department of Biological Engineering, Massachusetts Institute of Technology, Cambridge, Massachusetts; and [‖]Howard Hughes Medical Institute, Chevy Chase, Maryland

ABSTRACT Cell movement biased by a chemical gradient, or chemotaxis, coordinates the recruitment of cells and collective migration of cell populations. During wound healing, chemotaxis of fibroblasts is stimulated by platelet-derived growth factor (PDGF) and certain other chemoattractants. Whereas the immediate PDGF gradient sensing response has been characterized previously at the level of phosphoinositide 3-kinase (PI3K) signaling, the sensitivity of the response at the level of cell migration bias has not yet been studied quantitatively. In this work, we used live-cell total internal reflection fluorescence microscopy to monitor PI3K signaling dynamics and cell movements for extended periods. We show that persistent and properly aligned (i.e., high-fidelity) fibroblast migration does indeed correlate with polarized PI3K signaling; accordingly, this behavior is seen only under conditions of high gradient steepness (>10% across a typical cell length of 50 μm) and a certain range of PDGF concentrations. Under suboptimal conditions, cells execute a random or biased random walk, but nonetheless move in a predictable fashion according to the changing pattern of PI3K signaling. Inhibition of PI3K during chemotaxis is accompanied by loss of both cell-substratum contact and morphological polarity, but after a recovery period, PI3K-inhibited fibroblasts often regain the ability to orient toward the PDGF gradient.

INTRODUCTION

Chemotaxis is the most commonly encountered and best understood mechanism for directing cells to move from place to place. Eukaryotic cells sense chemoattractant gradients spatially, through a contrast in the occupancy of cell surface receptors and thus the levels of activated signaling molecules at the cell's front and rear (1). The requisite breaking of fore-aft symmetry is manifested in different ways depending on the cell type and mode of migration. In mesenchymal cells (e.g., fibroblasts), a broad, flat lamellipodium with newly formed adhesive contacts at its leading edge protrudes as a consequence of signaling pathways affecting actin polymerization. Nascent adhesions mature in response to actomyosin-dependent forces to form larger, more stable adhesions, which stall protrusion at the cell front and later disassemble. In contrast, amoeboid cells exhibit much faster protrusion of the cell front that is balanced by myosin-dependent squeezing forces at the rear. Intriguingly, some cell lineages and cancer cells adapt their behavior by transitioning between mesenchymal and amoeboid motility (2).

Cutaneous wound healing is marked by robust proliferation and chemotaxis of dermal fibroblasts, which follow gradients of platelet-derived growth factor (PDGF) and other clot-derived signals as they invade the wound as a population. In early studies, investigators assessed PDGF-stimulated chemotaxis of cultured fibroblasts by allowing cells to migrate across a porous membrane (Boyden chamber) (3). Such studies established the importance of phosphoinositide 3-kinase (PI3K)-dependent signaling (4,5), which is potently activated by PDGF receptors (6,7) courtesy of high-avidity binding of type IA PI3Ks (8). The Boyden chamber approach, however, is subject to known experimental and data interpretation difficulties (9), and as an endpoint assay it affords no opportunity to observe the cells as they move or to study the dynamic localization of intracellular signaling. We previously showed that PDGF gradients do in fact polarize PI3K signaling in fibroblasts (10), but with relatively low sensitivity (11). Whereas amoeboid cells are capable of robust morphological polarization and asymmetric intracellular signaling responses in shallow chemoattractant gradients (12,13), fibroblasts fail to do so unless the gradient of PDGF is well above 10% steepness across cellular dimensions. Although other studies have provided insights into the turning behavior of fibroblasts during chemotaxis (14,15), no work to date has directly related the spatiotemporal dynamics of intracellular signaling in individual fibroblasts to the fidelity of their long-term chemotactic responses. Therefore, it remains unclear whether the properties of the PDGF gradient sensing mechanism, which is manifested at the level of signaling through PI3K signaling, are indicative of the cells' overall chemotactic sensitivity. Alternatively, signaling to the cytoskeleton may be more sensitively amplified downstream of PI3K or in a parallel, PI3K-independent pathway.

The slow migration of fibroblasts (maximum speed ~1 μm/min) presents a challenge for long-term imaging

Submitted August 31, 2010, and accepted for publication February 22, 2011.

*Correspondence: jason_haugh@ncsu.edu

Editor: Andre Levchenko.

0006-3495/11/04/1893/9 $2.00

doi: 10.1016/j.bpj.2011.02.047

of gradient sensing and chemotaxis. In this study, we established stable PDGF gradients by inducing the slow release of PDGF from small (~20–60 μm diameter) alginate microspheres. Using total internal reflection fluorescence (TIRF) microscopy, we found that PI3K signaling and cell directionality are tightly correlated during fibroblast chemotaxis, consistent with previous analyses of random fibroblast migration (16). Additionally, we demonstrate that high-fidelity fibroblast chemotaxis is observed only when there is a steep gradient in PDGF receptor occupancy, which is tempered when the local PDGF concentration is sufficient to saturate receptor binding. Even when chemotactic fidelity is low, however, the directionality of migration is correlated with that of PI3K signaling polarity.

MATERIALS AND METHODS

Cell culture and reagents

Stable expression of the 3′ phosphoinositide-specific biosensor construct EGFP-AktPH in NIH 3T3 mouse fibroblasts (American Type Culture Collection) was established by retroviral infection as described previously (17). Cells were maintained in regular growth medium (Dulbecco's modified Eagle's medium supplemented with 10% v/v fetal bovine serum and 1% v/v penicillin/streptomycin/glutamate) in a 37°C, 5% CO_2 environment. All tissue culture reagents were purchased from Invitrogen (Carlsbad, CA), and cells were used between passages 10–40. The imaging buffer was 20 mM HEPES pH 7.4, 125 mM NaCl, 5 mM KCl, 1.5 mM $MgCl_2$, 1.5 mM $CaCl_2$, 10 mM glucose, and 2 mg/mL fatty acid-free bovine serum albumin, supplemented with 1% v/v fetal bovine serum. We obtained human plasma fibronectin from BD Biosciences (San Jose, CA), human recombinant PDGF-BB from Peprotech (Rocky Hill, NJ), and PI3K inhibitors from Calbiochem (San Diego, CA).

TIRF microscopy

TIRF microscopy was used to selectively excite fluorophores within ~100 nm of the cell-substratum contact area, effectively illuminating the plasma membrane and ~5–10% of the cytoplasm directly above it (18). Our prism-based TIRF microscope is described in detail elsewhere (11,17). A 60 mW, 488 nm line from a tunable wavelength argon ion laser head (Melles Griot, Irvine, CA) was used together with a 515/30 nm bandpass emission filter (Chroma, Brattleboro, VT), 20X and 10X water immersion objectives (Zeiss Achroplan), and a 0.63X camera mount. We acquired digital images at 2-min intervals using a Hamamatsu ORCA ER cooled CCD (Hamamatsu, Bridgewater, NJ) with a fixed exposure time multiplied by gain of 1000–1600 ms. Image acquisition was controlled with Metamorph imaging software (Universal Imaging, West Chester, PA).

Chemotaxis experiments

Cells were detached by a brief trypsin-EDTA treatment and then washed and resuspended in imaging buffer. Sterile glass coverslips were prepared by incubation with fibronectin (10 μg/mL coating concentration) for 60 min at 37°C, after which they were washed with deionized, sterile water and dried. Before imaging, 10^4 cells in 1 mL were added to each coverslip and allowed to spread for 2 h at 37°C. Sodium alginate microspheres were prepared as described previously (19) and mixed in a solution of 1 μM PDGF-BB (25 μL) for 24 h at 4°C. The microspheres were then washed three times with imaging buffer, and 50 μL of the bead suspension were added to the cells with 20 min remaining in the 2-h spreading period. The objective of the microscope was lowered into the buffer, and 200 μL of mineral oil were layered on top of the imaging buffer to prevent evaporation. Before TIRF imaging was performed, the positions of the beads were determined from a bright-field image, and the beads were similarly imaged at regular intervals during the experiment to confirm that they remained approximately stationary. When an inhibitor was added during the experiment, care was taken to avoid disturbing the beads.

The cells were allowed to migrate for 6–7 h, and those that met the following criteria were processed for analysis: 1), contact area $> 300\ \mu m^2$; 2), remained in the field of view and did not contact another cell during the experiment; and 3), showed significant displacement of the cell centroid.

Signaling vector analysis

Image segmentation and signaling vector analysis were carried out according to a previously described method (16,17). In brief, after an initial background subtraction, the pixels in each image are binned by fluorescence intensity via the k-means segmentation algorithm, with $k = 4$. So-called hot spots of PI3K signaling are identified as those contiguous regions, >20 pixels in size, that are assigned to the highest-intensity bin. After the area, A, average fluorescence intensity, F, and centroid position of each hot spot are determined, the signaling vector is calculated as follows: The coordinates of the cell's centroid are subtracted from those of each of its hot spots, i, defining the position of the hot spot relative to the cell centroid, $\mathbf{x_i} = (x_i, y_i)$, and its vector, $\mathbf{s}_i$, is defined with the magnitude equal to the fluorescence volume (A_iF_i). The overall resultant signaling vector, $\mathbf{S}$, is the vector sum of $\mathbf{s}_i$:

$$\mathbf{s}_i = A_iF_i \frac{\mathbf{x}_i}{\sqrt{x_i^2 + y_i^2}}; \quad \mathbf{S} = \sum_{i=1}^{N} \mathbf{s}_i \tag{1}$$

The cell migration vector, $\mathbf{C}$, is determined from the change in cell centroid position over a 12-min interval. The signaling vector $\mathbf{S}$ assigned to a particular cell movement step, from t_i to $t_i + 6\Delta t$, is taken as the average of $\mathbf{S}$ vectors calculated for t_i, $t_i + \Delta t$, . . ., $t_i + 5\Delta t$.

PDGF gradient calculations

During the period of observation, we expect a slow, quasi-steady release of ligand (PDGF) from each microsphere, with a roughly constant velocity (rate) per unit volume $v_{release}$, since PDGF that was contained in the bead but not physically bound to the alginate was presumably removed in the washing step. Clearly, this assumption is invalid for long incubation times, after the amount of bound PDGF has significantly decayed. As shown in Fig. S1 of the Supporting Material, we confirmed that the cell behavior remained consistent throughout the 6-h experiments. Under quasi-steady conditions, the flux at the surface, J_S, would satisfy

$$J_S = -D\frac{d[L]}{dr}\bigg|_{r=R_b} = \frac{R_b}{3} v_{release} \tag{2}$$

where $[L](r)$ is the concentration of the ligand in solution as a function of distance r from the center of the bead, D is its diffusivity, and R_b is the radius of the microsphere. If the surrounding medium were semi-infinite, the quasi-steady $[L](r)$ would simply scale as $1/r$; however, we need to account for the impermeable surface of the coverslip. To do this, we express the solution in Cartesian coordinates (x,y,z) and invoke the method of images (20). Thus, defining the surface as the $z = 0$ plane, we determine the relative distance, d_b, between any point $(x,y,0)$ and the center of the

bead (x_b,y_b,R_b), and calculate the ligand concentration field produced by each bead and the components of its gradient vector as follows:

$$\begin{aligned}
[L](x,y,0) &= \frac{2R_b^3 v_{release}}{3Dd_b};\\
\left.\frac{\partial[L]}{\partial x}\right|_{z=0} &= -(x-x_b)\left(\frac{R_b}{d_b}\right)^3\frac{2v_{release}}{3D};\\
\left.\frac{\partial[L]}{\partial y}\right|_{z=0} &= -(y-y_b)\left(\frac{R_b}{d_b}\right)^3\frac{2v_{release}}{3D};\\
d_b(x,y,0) &= \left[(x-x_b)^2+(y-y_b)^2+R_b^2\right]^{1/2}.
\end{aligned} \tag{3}$$

Next, assuming independent contributions from multiple beads and summing over them, and defining the PDGF gradient vector as **G**,

$$\begin{aligned}
[L](x,y,0) &= \frac{2v_{release}}{3D}\sum_{i=1}^{n}\frac{R_{b,i}^3}{d_{b,i}};\\
G_x &= -\frac{2v_{release}}{3D}\sum_{i=1}^{n}(x-x_{b,i})\left(\frac{R_{b,i}}{d_{b,i}}\right)^3;\\
G_y &= -\frac{2v_{release}}{3D}\sum_{i=1}^{n}(y-y_{b,i})\left(\frac{R_{b,i}}{d_{b,i}}\right)^3.
\end{aligned} \tag{4}$$

Hence, the properties of the gradient are calculated as follows: The normalized concentration of ligand, $[L]_{norm}$, is calculated according to Eq. 4, except without the presumably constant prefactor:

$$[L]_{norm}(x,y) = \sum_{i=1}^{n}\frac{R_{b,i}^3}{d_{b,i}} \tag{5}$$

The relative gradient, *RG*, of PDGF is determined from the magnitude of **G** as follows:

$$RG = \frac{\|\mathbf{G}\|}{[L]} \tag{6}$$

Here, the constant prefactor cancels out in the numerator and denominator.

Angle calculations

For each cell and time interval, the angles of the vectors **C**, **S**, and **G** (evaluated at the cell centroid), relative to the positive *x*-axis in the counterclockwise direction and set on a $(0,2\pi)$ scale, are determined by standard calculations. The angles between **C** and **G,** and between **S** and **G** are obtained by subtracting their respective angles and setting them on a $(-\pi,\pi)$ scale so that an angle of zero indicates that the two vectors are perfectly aligned.

Chemotactic and signaling indices

The chemotactic index (CI) is defined here as the ratio of overall movement projected in the direction of the PDGF gradient, **G** (which can change with time), to the total distance moved by the cell during the same time period. Consistent with the analyses described in the previous sections, **G** is evaluated at the cell centroid, and 12-min intervals are used for the cell movement vector, **C**. The CI is thus calculated as follows:

$$CI = \frac{\sum\limits_{\text{intervals } i}(\mathbf{C}\cdot\mathbf{G}/\|\mathbf{G}\|)_i}{\sum\limits_{\text{intervals } i}\|\mathbf{C}\|_i} \tag{7}$$

The signaling index (SI) is calculated by analogy to the CI in Eq. 7, but with **S** in place of **C**. Thus, the SI quantifies the overall tendency of the signaling vector to track the gradient.

RESULTS

Parallel observation of PI3K signaling dynamics and cell movement during fibroblast chemotaxis to PDGF

PI3K signaling was monitored in migrating NIH 3T3 fibroblasts expressing the EGFP-AktPH biosensor, illuminated in the cell-substratum contact area by TIRF microscopy. To stimulate their chemotaxis, PDGF gradients were formed by slow release and diffusion from alginate beads, which act as electrostatic sponges for basic proteins such as PDGF-BB (21). The normalized PDGF concentration profile, $[L]_{norm}$, and concentration gradient vector, **G**, were calculated based on the assumption that PDGF is released at a constant rate per unit volume within each bead (see Materials and Methods). Thus, the midpoint concentration and magnitude of the PDGF gradient seen by each cell depend on the positions and sizes of the nearby bead(s) (Fig. 1 *a*). Larger beads produce higher concentrations, and the presence of multiple beads near a cell tends to increase the concentration while tempering the gradient steepness.

An advantage of our prism-based TIRF microscope, as compared with commercially available, objective-based microscopes, is its ability to image cells at lower magnification, which is suitable for tracking cells over 6–7 h. Still, the spatial resolution (~1 μm) is sufficient to image localized hot spots of intense PI3K signaling, which are consistently localized in protruding lamellipodia (Fig. 1 *b* and Movie S1). As described previously in the context of random migration (16,17), we quantify the orientation of a cell's PI3K signaling pattern in terms of a signaling vector, which accounts for the positions of the hot spots relative to the centroid and their relative sizes and intensities.

To quantify the fidelity of chemotactic migration and signaling as a function of time, we calculate the angles between the vector of cell centroid movement, **C**, and the PDGF gradient vector, **G**, and between the PI3K signaling vector, **S**, and **G**. A value of zero indicates perfect alignment with the chemoattractant gradient. An examination of one of the most persistently aligned cell migration paths demonstrates that the cell is capable of turning so as to track the direction in which the PDGF gradient is steepest, with PI3K signaling consistently polarized in the direction of migration (Fig. 1 *c*). A total of 54 cells were analyzed in this fashion. The cells did not execute apparent taxis in control experiments performed with mock-prepared beads, in the absence of PDGF (results not shown).

Chemotactic fibroblasts exhibit periods of persistently polarized signaling and smooth crawling, interspersed with periods of stochastic signaling and membrane protrusion

During random migration, mesenchymal cells (e.g., fibroblasts) often exhibit multiple lamellipodia that protrude in

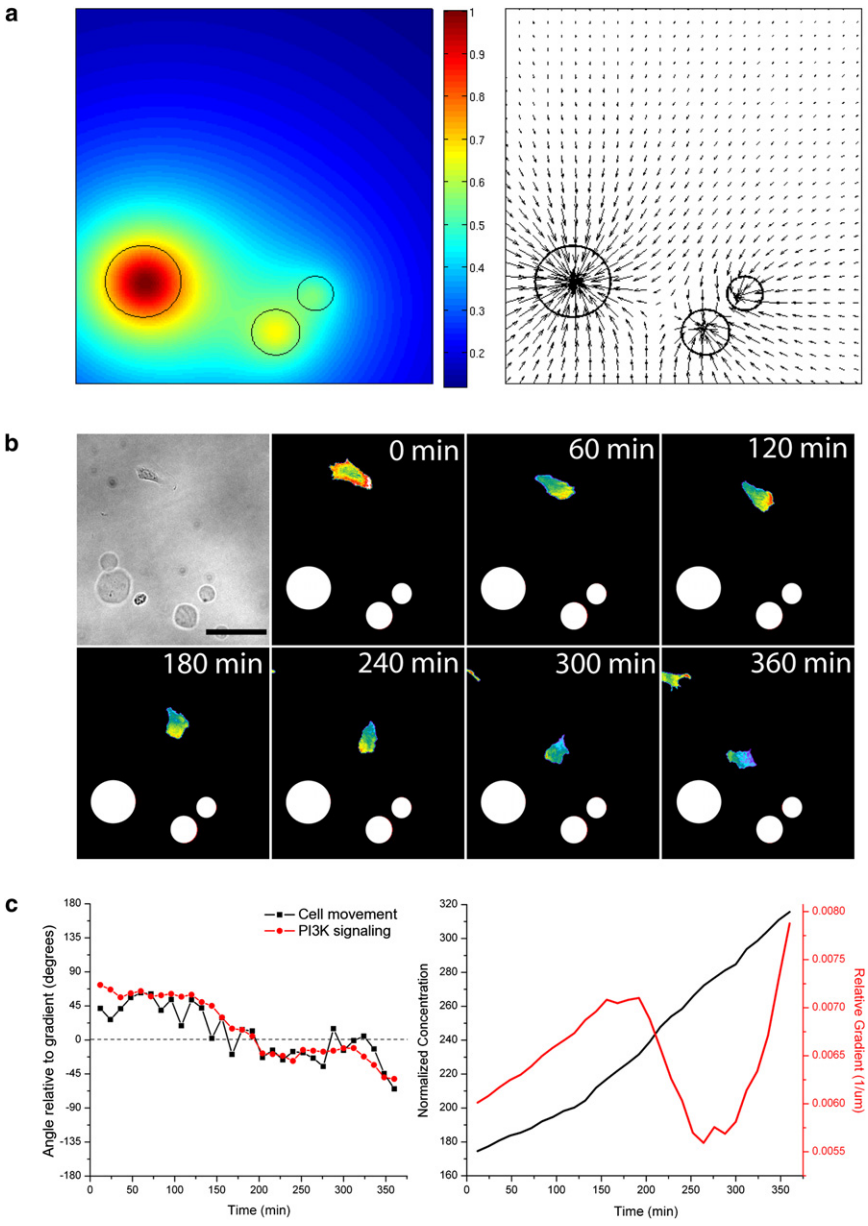

FIGURE 1 Generation of chemotactic PDGF gradients by slow release from alginate microspheres. (*a*) The two plots show maps of the calculated PDGF concentration (*left panel*, normalized by the maximum value) and PDGF gradient vector (*right panel*, magnitude indicated by arrow length) evaluated at the surface of the coverslip ($z = 0$). PDGF-loaded microsphere locations and diameters are indicated by open circles. (*b*) Montage of a GFP-AktPH-expressing NIH 3T3 mouse fibroblast migrating chemotactically toward the PDGF gradient field depicted in *A*. The bright-field image in the top left corner shows the cell in relation to the PDGF-loaded microspheres; scale bar = 70 μm. The other panels show the time course of cell contact area translocation and relative PI3K signaling gradient, monitored by TIRF microscopy and displayed using a pseudo-color intensity scale (see also Movie S1). (*c*) Metrics of chemotactic fidelity for the cell in *b*. Cell movement and PI3K signaling vector orientations, expressed as angles relative to the PDGF gradient vector (*left panel*), and the normalized PDGF concentration and relative gradient (*RG*) evaluated at the cell centroid (*right panel*), are plotted as a function of time.

different directions, whereas cells that move more persistently have an elongated morphology with a single, larger lamellipodium. These two random migration phenotypes have been quantitatively characterized by analogy to the run-and-tumble swimming of motile bacteria (22). In our cells, PI3K signaling was in both cases localized in protrusive structures (17).

In fibroblasts that migrate in PDGF gradients, productive chemotaxis is similarly interrupted by periods of conflicted migration, characterized by cell morphologies with multiple protrusions (Fig. 2 *a* and Movie S2). As in randomly migrating fibroblasts, these structures protrude and harbor intense PI3K signaling in an intermittent fashion. Accordingly, the cell centroid moves in a zigzag path as compared with periods of persistent crawling, quantified in terms of the cell migration angle versus time (Fig. 2 *b*). Nevertheless, under favorable conditions, such cells make steady progress in the direction of increasing PDGF concentration.

Robust fibroblast chemotaxis requires steep PDGF gradients and is sensitive to the PDGF concentration

To further characterize the chemotactic behavior of each cell in relation to the PDGF gradient it experienced, we calculated the absolute value of the cell migration angle relative to the PDGF gradient for each time interval and binned its value according to movement toward the gradient (0–60°, *red*), orthogonal to the gradient (60–120°, *white*), or away from the gradient (120–180°, *blue*). A pile-up of these

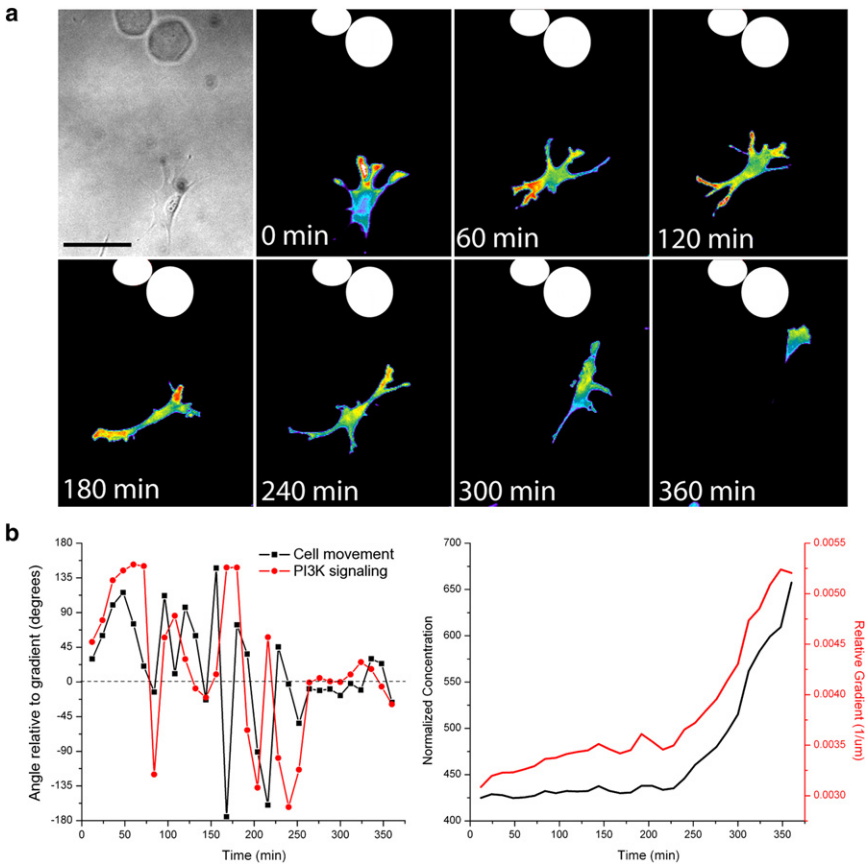

FIGURE 2 Morphological characteristics of fibroblasts exhibiting conflicted versus persistent chemotaxis behaviors. (*a*) The bright-field image in the top left corner shows the cell in relation to the PDGF-loaded microspheres; scale bar = 70 μm. The other panels show the time course of cell contact area translocation and relative PI3K signaling gradient, monitored by TIRF microscopy and displayed using a pseudo-color intensity scale (see also Movie S2). (*b*) Metrics of chemotactic fidelity for the cell in *a*. Cell movement and PI3K signaling vector orientations, expressed as angles relative to the PDGF gradient vector (*left panel*), and the normalized PDGF concentration and relative gradient (*RG*) evaluated at the cell centroid (*right panel*), are plotted as a function of time.

angle maps allows one to visualize the behavior of all 54 cells as a population, ranked and segmented into three subpopulations of high, intermediate, and low chemotactic fidelity according to a simple score (number of red intervals minus the number of blue intervals; Fig. 3 *a*). Plots showing the centroid paths of cells (with the initial PDGF gradient oriented along the positive x axis) in each of the three subpopulations confirm that the migration paths range from predominantly tactic to predominantly random (Fig. 3 *b*).

We previously showed that robust polarization of PI3K signaling stimulated by PDGF gradients in fibroblasts requires high gradient steepness and intermediate PDGF concentrations (11). High concentrations of PDGF-BB (>10 nM) produce maximal PI3K signaling but uniformly saturate the receptors on the cell surface.

To evaluate whether these trends carry over to the migration response, we plotted each cell in the cohort according to its mean relative gradient steepness and mean PDGF concentration (*RG* and $[L]_{norm}$, respectively; see Materials and Methods), evaluated at its centroid (Fig. 3 *c*). For the purpose of comparison, relative gradients of 0.001/μm and 0.01/μm correspond to gradients of 5% and 50%, respectively, across a typical cell length of 50 μm. The values of both *RG* and $[L]_{norm}$ naturally varied across ~1.5 logs. To indicate the corresponding migration behavior, the data point for each cell was color-coded according to whether it was grouped in the high-, intermediate-, or low-fidelity subpopulation.

This analysis revealed that high chemotactic fidelity does indeed require a steep PDGF gradient. All of the cells in the high-fidelity subpopulation saw PDGF gradients with mean $RG > 0.002/\mu$m, or a >10% difference across 50 μm. The results further show that the highest PDGF concentrations do not promote high-fidelity chemotaxis, even when the gradient is steep, consistent with receptor saturation. Although it is difficult to attain gradients with low concentration and high relative steepness by the method used, the cells should not be able to respond to vanishingly small PDGF concentrations either.

PDGF-directed fibroblast migration varies in chemotactic fidelity but nonetheless correlates with PI3K signaling pattern

Having characterized the directionally biased movements of the cells, we sought to assess the extent to which those movements correlate with the polarization of PI3K signaling. To that end, we applied two different analyses. First, we constructed a frequency density map of signaling

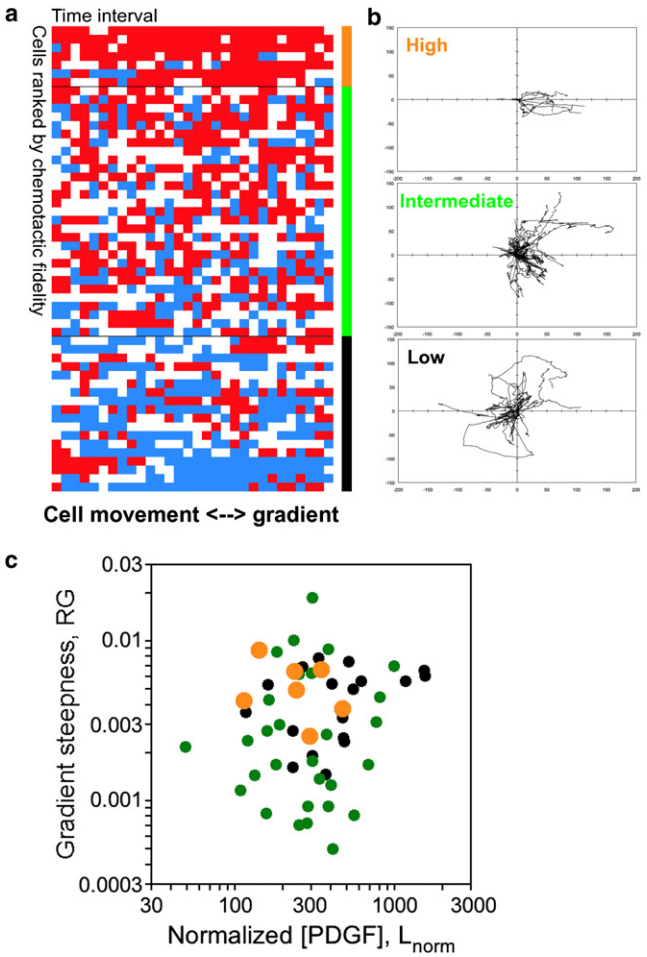

FIGURE 3 Characterization of chemotactic fidelity and relation to PDGF gradient properties. (*a*) The absolute value of the cell movement vector orientation angle, relative to the PDGF gradient vector, is color-coded for each cell and time interval: red, 0–60°; white, 60–120°; blue, 120–180°. The 54 cells are sorted according to the number of red intervals minus the number of blue intervals and grouped by that score into high, intermediate, and low subpopulations using the *k*-means algorithm. (*b*) Cell centroid translocation paths for the three cell subpopulations grouped in *a*, with the initial centroid positions located at the origin and the initial PDGF gradient vector aligned along the positive *x* axis. (*c*) For each of the 54 cells, the mean values of the relative gradient steepness (*RG*) and normalized ligand concentration ($[L]_{norm}$) are indicated, as is the membership of each cell in the high- (*orange*), intermediate- (*green*), or low- (*black*) fidelity subpopulation.

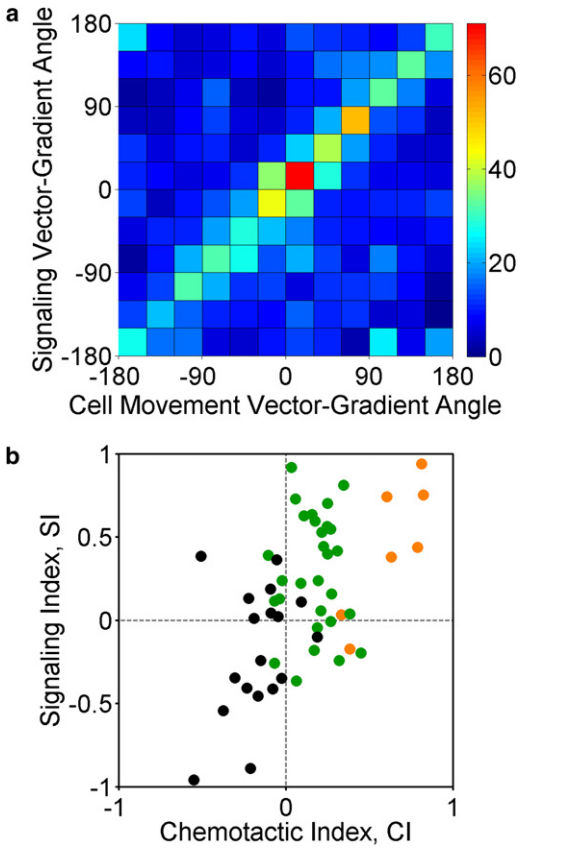

FIGURE 4 The fidelity of chemotactic cell movement correlates with the orientation of PI3K signaling. (*a*) Density map of the PI3K signaling vector-PDGF gradient angle versus the cell movement vector-PDGF gradient angle, both expressed in degrees. An angle of zero indicates perfect alignment with the PDGF gradient. All time intervals (for the same 54 cells as in Fig. 3) are pooled. Density is given as the absolute number of instances in each square. (*b*) Dot plot of SI versus CI for each of the 54 cells.

vector to gradient angle versus cell movement vector-gradient angle for all time intervals (Fig. 4 *a*); thus, the measurements acquired for all of the cells were pooled. The plot shows that the highest density is close to the origin, confirming that the most common tendency of the cell population is to align both PI3K signaling and net movement in the direction of the PDGF gradient. Moreover, the plot shows intermediate density along the $y = x$ diagonal and at the corners. This indicates that when the cell is not properly aligned toward the gradient, the PI3K signaling pattern and net cell movement tend to adopt similarly misaligned orientations. A qualitative comparison of the frequency density maps for the first and last 3 h of the experiment confirms that the relationship between signaling and migration remained consistent throughout the 6-h experiments (Fig. S1). For each cell, a cross-correlation of its signaling and movement angles with variable time shift showed a positive correlation near zero time shift, with the breadth of the peak reflecting the temporal persistence of the two responses (Fig. S2).

Second, we correlated metrics designed to evaluate the overall chemotaxis and PI3K signaling orientation of each individual cell: the CI and an analogous quantity, the SI (see Materials and Methods). Although the CI is commonly used to quantify chemotactic fidelity, our definition differs somewhat in that it allows for changes in the orientation of the two-dimensional gradient field as the location of the cell centroid changes. Fig. 4 *b* shows a dot plot of SI versus CI for each cell. It is color-coded as in Fig. 3 and thus shows that the scoring of the cells based on migration angle versus time almost perfectly bins the cells according to their CI

values arranged along the abscissa. Over the range of values, SI and CI are positive correlated (correlation coefficient = 0.55, $p = 2 \times 10^{-5}$), indicating that the PI3K signaling pattern and net movement tend to be coaligned even in cells that migrate with low fidelity to the gradient.

Of note, a group of cells exhibited high polarization of PI3K hot spots (SI > 0.5) but only modestly positive CI (Fig. 4 *b*). Further analysis revealed that many of these cells saw shallow relative gradients with not-too-high midpoint PDGF concentrations (Fig. S3), suggesting that symmetry breaking of PI3K hot-spot localization may be more responsive to shallow gradients than is the chemotactic response. We detected no such sensitivity in our previous analysis (11), which systematically avoided hot spots and did not allow for repolarization of the cell morphology after application of the PDGF gradient.

Rapid inhibition of PI3K signaling depolarizes chemotaxing fibroblasts, after which the cells typically recover the ability to properly orient toward the PDGF gradient

In fibroblasts, PI3K signaling is generally localized in protruding membrane structures; however, it remains to be established that this is functionally relevant and not simply a correlated by-product of other localized signaling processes. Although inhibition of PI3Ks or mutation of the PI3K-binding sites on PDGF receptors diminishes fibroblast chemotaxis through a porous membrane (the Boyden chamber assay) (4,5), recent studies of amoeboid cell chemotaxis have suggested that the importance and role(s) of PI3K signaling in directed migration are highly context-dependent (23–26).

EGFP-AktPH-expressing cells ($n = 30$) were allowed to migrate in PDGF gradients for ~4 h, after which they were treated with one of two PI3K inhibitors: LY294002 (100 μM) or the more potent and selective PI3Kα inhibitor IV (3 μM). Thereafter, the cells generally exhibited a dramatic decrease in TIRF intensity and cell motility, with the cell contact area adopting a rounded-up morphology. Of these cells, more than half ($n = 17$) later showed a partial recovery of their contact areas but not of their PI3K signaling, and did not fully resume their normal crawling morphologies (Fig. 5, *a* and *b*). The apparent adhesion defect is consistent with our previous measurements of fibroblast spreading velocities in control versus PI3K-inhibited cells (17). Despite these indications, those cells that recovered adhesion largely maintained their individual tendencies to move toward the PDGF gradient, as judged by a comparison of their CI values before and after PI3K inhibition, and instances in which the CI markedly improved after inhibitor treatment are noteworthy (Fig. 5 *c*). In accord with our previous study of fibroblast spreading (17), as well as studies of amoeboid chemotaxis by other investigators (23–26), these results suggest that PI3K signaling is important for integrating certain motility processes but is not absolutely required for fibroblast chemotaxis.

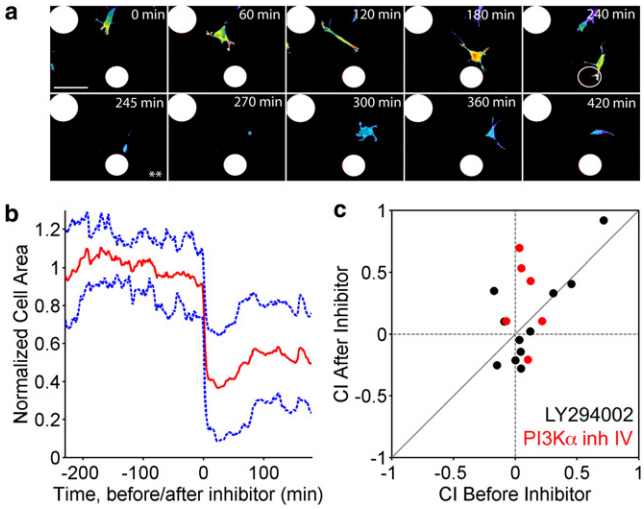

FIGURE 5 PI3K inhibition depolarizes chemotaxing fibroblasts, but they are capable of reorienting thereafter. GFP-AktPH-expressing NIH 3T3 cells were monitored by TIRF microscopy as they migrated in the vicinity of PDGF-loaded microspheres (positions and sizes as indicated). After ~4 h, one of two PI3K inhibitors was added, and the cells were observed for an additional 3 h. After 17 out of 30 cells experienced a marked cringe response to inhibitor addition, they exhibited partial recovery of adhesion by respreading and were analyzed further. (*a*) Pseudo-color montage of a representative cell treated with LY294002 after 240 min; scale bar = 70 μm (see also Movie S3). (*b*) Time course of cell contact area, normalized by each cell's time-averaged contact area before inhibition, showing the dramatic loss and partial recovery of adhesion by these cells (mean ± SD, $n = 17$). (*c*) Comparison of CI values post- and pre-inhibition for each cell in the population.

DISCUSSION

Localization of PI3K-dependent signaling pathways is apparently important for cell migration in many but not all cell/environmental contexts (27). Here, using TIRF microscopy, we showed that fibroblasts respond to PDGF gradients with correlated PI3K signaling and biased migration responses, and exhibit robust chemotactic fidelity only for certain gradient conditions. Cells that are located too close to a large bead might see a saturating concentration of PDGF, whereas very distant cells have difficulty sensing what would be a shallow PDGF gradient. Thus, cells that are moderately close to a smaller bead apparently are exposed to more favorable chemotactic gradients, which are sufficiently steep (>10% across the cell) without saturating cell surface receptors. These results suggest that the efficiency of fibroblast chemotaxis is limited by the modest sensitivity of the previously characterized PDGF receptor/PI3K gradient sensing module (11) and of other PDGF receptor-mediated signaling pathways. In vivo, the collective invasion of fibroblasts can be maintained through

cell-mediated erosion of the PDGF gradient (28). Thus, the ability to produce a sufficiently steep gradient would depend on the cell density, an example of quorum sensing.

PI3K signaling is strikingly localized in protruding lamellipodia during both random and chemotactic fibroblast migration, which indicates that 3′ phosphoinositides are generally involved in fibroblast motility or in cell functions that need to be spatiotemporally coordinated with motility. This is not to say that PI3K-dependent signaling is the sole controller of gradient sensing and polarized movement, especially considering that these might be distinct processes (14,29,30). In fibroblasts, Rac and other Rho-family GTPases play various roles in regulating protrusion, cell speed, and persistence (31,32), and have been implicated in PDGF-stimulated chemotaxis (15,33). Complicating such matters is the ample evidence that Rho-family GTPases can be activated through both PI3K-dependent and -independent pathways, and that PI3K signaling can control actin polymerization independently from small GTPases (34–36). Indeed, our inhibitor results (Fig. 5) suggest that PI3K signaling plays a role in mediating differential adhesion and/or other leading-edge dynamics, rather than serving as the sole determinant of cell orientation. Our observation that some cells persistently polarized their PI3K signaling (as judged by a high positive value of SI) but failed to chemotax efficiently further underscores the need to characterize the integration of PI3K signaling with other promotility pathways.

In mesenchymal cell migration in particular, signaling networks mediated by growth factor receptors are superimposed on those of integrins, and the dynamics of adhesions and cytoskeletal structures are intimately coupled (37). Indeed, in the context of fibroblast migration on fibronectin, we previously characterized the dynamics of PI3K signaling and its relation to the directional persistence of random migration (16). A quantitative analysis revealed that signaling in spatially distant regions of the cell are subject to stochastic fluctuations that are globally coupled, such that the pattern of signaling is metastable. Hence, the following fundamental question arises: Does graded chemoattractant receptor signaling bias migration by exceeding the noise associated with random migration signaling (14,38,39), or does it suppress noise by global inhibition (40)? The aforementioned global coupling of PI3K signaling dynamics in randomly migrating fibroblasts, together with the saturable PI3K recruitment by PDGF receptors in this system (11,41), implicates the latter mechanism. These lines of evidence further suggest that the mechanism of global inhibition is competition for a limiting pool of PI3K; however, such a suppression mechanism would be ineffective at the lower limit of gradient detection (39). We therefore speculate that the PDGF gradient criteria required for high-fidelity chemotaxis might be less demanding at lower levels of adhesion-based signaling, but at the expense of overall cell speed.

Finally, we observe that the microsphere depot approach for generating chemotactic gradients (in conjunction with microscopic observation of the cells) has several advantages and also a notable limitation. The method is simple to implement and avoids the stability issues associated with flow from a micropipette, and it can produce sharper gradients than can typically be achieved with diffusion-based microfluidic chambers. The limitation, however, is that the kinetics of release are governed by the noncovalent interactions of the chemoattractant within the microsphere, and therefore the common approach of using a volume-filling dye (fluorescent dextran, for example) as a proxy to estimate the typically low absolute concentrations of the chemoattractant is not viable.

SUPPORTING MATERIAL

Three figures and three movies are available at http://www.biophysj.org/biophysj/supplemental/S0006-3495(11)00298-0.

This work was supported by the National Science Foundation (0828936) and the National Institutes of Health (GM074711). Y.W. and D.J.I. were supported by the National Institutes of Health (EB007280). D.J.I. is an investigator of the Howard Hughes Medical Institute.

REFERENCES

1. Ridley, A. J., M. A. Schwartz, …, A. R. Horwitz. 2003. Cell migration: integrating signals from front to back. *Science.* 302:1704–1709.
2. Friedl, P., and K. Wolf. 2010. Plasticity of cell migration: a multiscale tuning model. *J. Cell Biol.* 188:11–19.
3. Seppä, H., G. Grotendorst, …, G. R. Martin. 1982. Platelet-derived growth factor in chemotactic for fibroblasts. *J. Cell Biol.* 92:584–588.
4. Kundra, V., J. A. Escobedo, …, B. R. Zetter. 1994. Regulation of chemotaxis by the platelet-derived growth factor receptor-β. *Nature.* 367:474–476.
5. Wennström, S., A. Siegbahn, …, L. Claesson-Welsh. 1994. Membrane ruffling and chemotaxis transduced by the PDGF β-receptor require the binding site for phosphatidylinositol 3′ kinase. *Oncogene.* 9:651–660.
6. Auger, K. R., L. A. Serunian, …, L. C. Cantley. 1989. PDGF-dependent tyrosine phosphorylation stimulates production of novel polyphosphoinositides in intact cells. *Cell.* 57:167–175.
7. Jackson, T. R., L. R. Stephens, and P. T. Hawkins. 1992. Receptor specificity of growth factor-stimulated synthesis of 3-phosphorylated inositol lipids in Swiss 3T3 cells. *J. Biol. Chem.* 267:16627–16636.
8. Barua, D., J. R. Faeder, and J. M. Haugh. 2008. Computational models of tandem SRC homology 2 domain interactions and application to phosphoinositide 3-kinase. *J. Biol. Chem.* 283:7338–7345.
9. Zigmond, S. H., and J. G. Hirsch. 1973. Leukocyte locomotion and chemotaxis. New methods for evaluation, and demonstration of a cell-derived chemotactic factor. *J. Exp. Med.* 137:387–410.
10. Haugh, J. M., F. Codazzi, …, T. Meyer. 2000. Spatial sensing in fibroblasts mediated by 3′ phosphoinositides. *J. Cell Biol.* 151:1269–1280.
11. Schneider, I. C., and J. M. Haugh. 2005. Quantitative elucidation of a distinct spatial gradient-sensing mechanism in fibroblasts. *J. Cell Biol.* 171:883–892.
12. Servant, G., O. D. Weiner, …, H. R. Bourne. 2000. Polarization of chemoattractant receptor signaling during neutrophil chemotaxis. *Science.* 287:1037–1040.
13. Janetopoulos, C., L. Ma, …, P. A. Iglesias. 2004. Chemoattractant-induced phosphatidylinositol 3,4,5-trisphosphate accumulation is

spatially amplified and adapts, independent of the actin cytoskeleton. *Proc. Natl. Acad. Sci. USA*. 101:8951–8956.

14. Arrieumerlou, C., and T. Meyer. 2005. A local coupling model and compass parameter for eukaryotic chemotaxis. *Dev. Cell.* 8:215–227.
15. Monypenny, J., D. Zicha, …, N. Watanabe. 2009. Cdc42 and Rac family GTPases regulate mode and speed but not direction of primary fibroblast migration during platelet-derived growth factor-dependent chemotaxis. *Mol. Cell. Biol.* 29:2730–2747.
16. Weiger, M. C., S. Ahmed, …, J. M. Haugh. 2010. Directional persistence of cell migration coincides with stability of asymmetric intracellular signaling. *Biophys. J.* 98:67–75.
17. Weiger, M. C., C.-C. Wang, …, J. M. Haugh. 2009. Spontaneous phosphoinositide 3-kinase signaling dynamics drive fibroblast spreading and random migration. *J. Cell Sci.* 122:313–323.
18. Schneider, I. C., and J. M. Haugh. 2004. Spatial analysis of 3′ phosphoinositide signaling in living fibroblasts: II. Parameter estimates for individual cells from experiments. *Biophys. J.* 86:599–608.
19. Phee, H., I. Dzhagalov, …, A. Weiss. 2010. Regulation of thymocyte positive selection and motility by GIT2. *Nat. Immunol.* 11:503–511.
20. Deen, W. M. 1998. Analysis of Transport Phenomena. Oxford University Press, New York.
21. Liao, I. C., A. C. Wan, …, K. W. Leong. 2005. Controlled release from fibers of polyelectrolyte complexes. *J. Control. Release.* 104:347–358.
22. Potdar, A. A., J. Lu, …, P. T. Cummings. 2009. Bimodal analysis of mammary epithelial cell migration in two dimensions. *Ann. Biomed. Eng.* 37:230–245.
23. Kay, R. R., P. Langridge, …, O. Hoeller. 2008. Changing directions in the study of chemotaxis. *Nat. Rev. Mol. Cell Biol.* 9:455–463.
24. Kölsch, V., P. G. Charest, and R. A. Firtel. 2008. The regulation of cell motility and chemotaxis by phospholipid signaling. *J. Cell Sci.* 121:551–559.
25. Heit, B., L. X. Liu, …, P. Kubes. 2008. PI3K accelerates, but is not required for, neutrophil chemotaxis to fMLP. *J. Cell Sci.* 121:205–214.
26. Yoo, S. K., Q. Deng, …, A. Huttenlocher. 2010. Differential regulation of protrusion and polarity by PI3K during neutrophil motility in live zebrafish. *Dev. Cell.* 18:226–236.
27. Cain, R. J., and A. J. Ridley. 2009. Phosphoinositide 3-kinases in cell migration. *Biol. Cell.* 101:13–29.
28. Haugh, J. M. 2006. Deterministic model of dermal wound invasion incorporating receptor-mediated signal transduction and spatial gradient sensing. *Biophys. J.* 90:2297–2308.
29. Devreotes, P., and C. Janetopoulos. 2003. Eukaryotic chemotaxis: distinctions between directional sensing and polarization. *J. Biol. Chem.* 278:20445–20448.
30. Stephens, L., L. Milne, and P. Hawkins. 2008. Moving towards a better understanding of chemotaxis. *Curr. Biol.* 18:R485–R494.
31. Pankov, R., Y. Endo, …, K. M. Yamada. 2005. A Rac switch regulates random versus directionally persistent cell migration. *J. Cell Biol.* 170:793–802.
32. Machacek, M., L. Hodgson, …, G. Danuser. 2009. Coordination of Rho GTPase activities during cell protrusion. *Nature.* 461:99–103.
33. Hooshmand-Rad, R., L. Claesson-Welsh, …, C. H. Heldin. 1997. Involvement of phosphatidylinositide 3′-kinase and Rac in platelet-derived growth factor-induced actin reorganization and chemotaxis. *Exp. Cell Res.* 234:434–441.
34. Oikawa, T., H. Yamaguchi, …, T. Takenawa. 2004. PtdIns(3,4,5)P3 binding is necessary for WAVE2-induced formation of lamellipodia. *Nat. Cell Biol.* 6:420–426.
35. Primo, L., L. di Blasio, …, F. Bussolino. 2007. Essential role of PDK1 in regulating endothelial cell migration. *J. Cell Biol.* 176:1035–1047.
36. Inoue, T., and T. Meyer. 2008. Synthetic activation of endogenous PI3K and Rac identifies an AND-gate switch for cell polarization and migration. *PLoS ONE.* 3:e3068.
37. Vicente-Manzanares, M., C. K. Choi, and A. R. Horwitz. 2009. Integrins in cell migration—the actin connection. *J. Cell Sci.* 122:199–206.
38. Tranquillo, R. T., D. A. Lauffenburger, and S. H. Zigmond. 1988. A stochastic model for leukocyte random motility and chemotaxis based on receptor binding fluctuations. *J. Cell Biol.* 106:303–309.
39. van Haastert, P. J., and M. Postma. 2007. Biased random walk by stochastic fluctuations of chemoattractant-receptor interactions at the lower limit of detection. *Biophys. J.* 93:1787–1796.
40. Iglesias, P. A., and P. N. Devreotes. 2008. Navigating through models of chemotaxis. *Curr. Opin. Cell Biol.* 20:35–40.
41. Park, C. S., I. C. Schneider, and J. M. Haugh. 2003. Kinetic analysis of platelet-derived growth factor receptor/phosphoinositide 3-kinase/Akt signaling in fibroblasts. *J. Biol. Chem.* 278:37064–37072.